Ullal et al., http://www.jcb.org/cgi/content/full/jcb.201504073/DC1

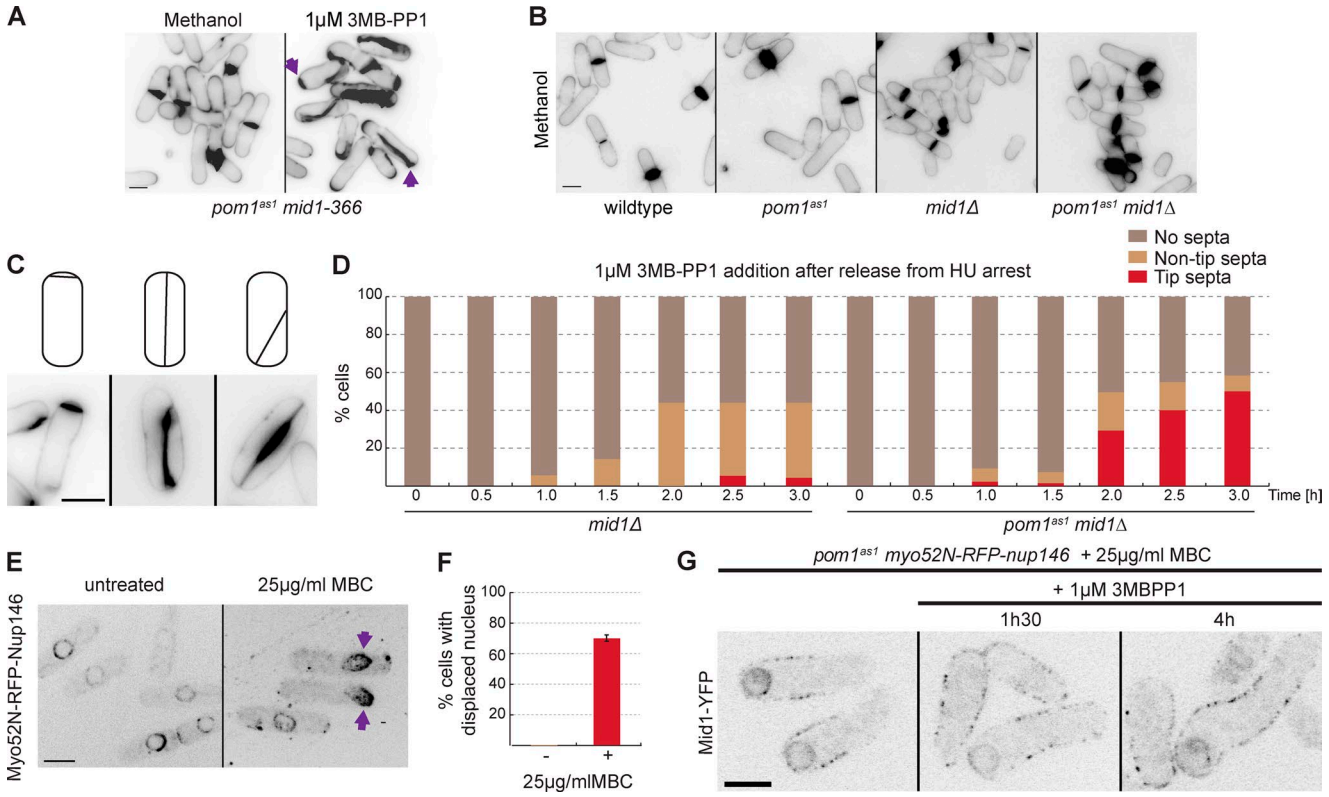

Figure S1. **Pom1 kinase activity is required to prevent division septum assembly at cell tips.** (A) Calcofluor images of *pom1^{as1} mid1-366* cells treated with methanol or 3MB-PP1 for 2 h at 25°C. Arrowheads indicate tip septa. (B) Images of cells of indicated genotypes treated with methanol (control) at 25°C for 2 h and stained with calcofluor. See Fig. 1 (A and B), for corresponding 3MB-PP1–treated cells and quantification. (C) Classes of tip septa observed in *pom1^{as1} mid1Δ* after treatment with 1 µM 3MB-PP1 for 2 h at 25°C. (D) Quantification of septal phenotypes in *mid1Δ* and *pom1^{as1} mid1Δ* cells synchronized in S-phase at 25°C by incubation in hydroxyurea for 6 h. After hydroxyurea (HU) washout, 1 µM 3MB-PP1 was added. At indicated time points, cells were stained with calcofluor and medial and tip septa quantified (n > 200). (E) Myo52N-RFP-Nup146 localization showing nuclear displacement in *nmt81::myo52N-RFP-nup146* cells treated with 25 µg/ml MBC for 4 h. (F) Quantification of nuclear displacement in cells as in E (n > 100). (G) Mid1-YFP localization in *pom1^{as1} nmt81::myo52N-RFP-nup146* cells treated with 25 µg/ml MBC to displace the nucleus, and untreated or treated for 1 h, 30 min, or 4 h with 1 µM 3MBPP1 to inactivate Pom1^{as1}. Error bars are standard deviation. Bars, 5 µm.

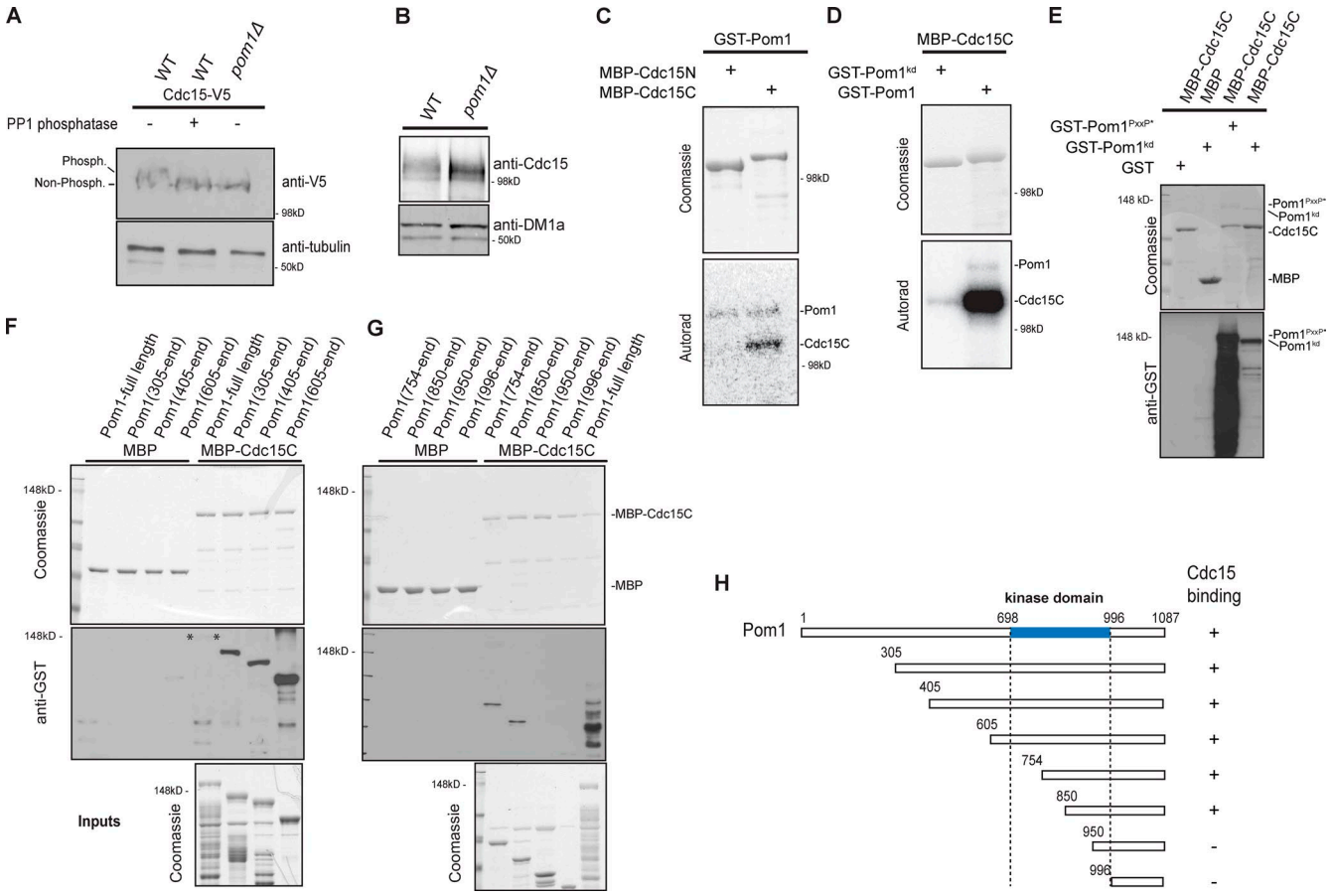

Figure S2. **Pom1 phosphorylates and binds the F-BAR protein Cdc15.** (A) Cdc15 is phosphorylated in a Pom1 dependent manner in vivo. Cdc15-V5 with (+) or without (–) PP1 phosphatase treatment in wild-type and *pom1Δ* strains was detected with the anti-V5 HRP antibody. Tubulin was used as loading control. (B) Cdc15 in wild-type and *pom1Δ* strains detected with anti-Cdc15 serum. DM1a was used as loading control. (C) In vitro kinase assays performed with purified, recombinant GST-Pom1, and recombinant MBP-Cdc15N and MBP-Cdc15C. Bottom panel shows Phosphorimager detection of ^{32}P incorporation and top panel shows Coomassie-stained gels of substrates input. (D) In vitro kinase assays performed with purified, recombinant GST-Pom1 or GST-Pom1^{kd} and recombinant MBP-Cdc15C. Bottom panel shows Phosphorimager detection of ^{32}P incorporation, and top panel shows Coomassie-stained gels of substrates input. (E) In vitro binding assays between Pom1 and Cdc15 using recombinant MBP and MBP-Cdc15C incubated with recombinant GST, GST- *Pom1^{PxxP*}* and GST-Pom1^{kd}. Amylose beads were washed, and bound proteins were run on SDS-PAGE and detected by Coomassie staining (top) and anti-GST antibodies (bottom). (F and G) In vitro binding assays between Pom1 truncations and Cdc15 using recombinant MBP and MBP-Cdc15C incubated with the recombinant GST-Pom1 truncations indicated. Amylose beads were washed and bound proteins were run on SDS-PAGE and detected by Coomassie staining (top) and anti-GST antibodies (bottom). One fifth of each GST fragment input is shown as a control. (H) Schematic representation of Pom1 fragments used and indication of Cdc15 binding.

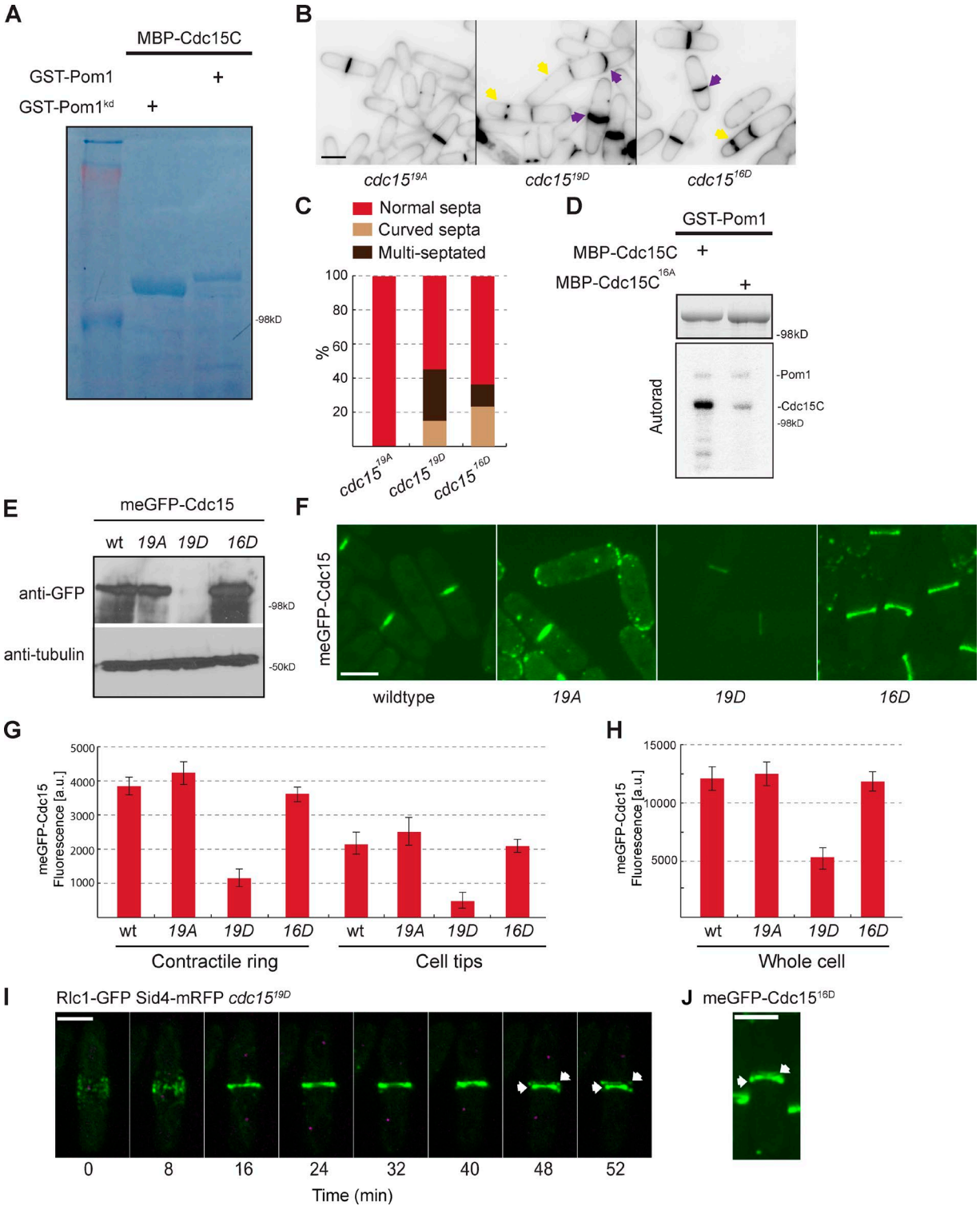

Figure S3. **Pom1 phosphorylates Cdc15 to prevent septum formation at cell tips.** (A) Cold in vitro kinase assay performed with recombinant MBP-Cdc15C and purified, recombinant GST-Pom1^{kd} or GST-Pom1. These fragments were TCA precipitated and analyzed by mass spectrometry to determine the phosphorylated sites. (B) Images of *cdc15^{19A}*, *cdc15^{19D}* and *cdc15^{16D}* cells stained with calcofluor. Yellow arrows indicate multiseptated cells and purple arrows indicate cells with curved septa. (C) Quantification of septa in septated cells as in C (n > 100). (D) In vitro kinase assays performed with purified recombinant GST-Pom1 and recombinant wild-type MBP-Cdc15C and MBP-Cdc15C^{16A} fragments. Phosphorimager detection of ^{32}P incorporation (bottom) and Coomassie-stained gels of substrates input (top) are shown. (E) meGFP-Cdc15, meGFP-*cdc15^{19A}*, meGFP-*cdc15^{19D}*, and meGFP-*cdc15^{16D}* were detected by Western blotting using anti-GFP antibodies. Tubulin is used as loading control. (F) Images of meGFP-Cdc15, meGFP-*cdc15^{19A}*, meGFP-*cdc15^{19D}*, and meGFP-*cdc15^{16D}*. (G and H) Quantification of GFP intensity at tips, cytokinetic rings, and whole cells in meGFP-Cdc15, meGFP-*cdc15^{19A}*, meGFP-*cdc15^{19D}*, and meGFP-*cdc15^{16D}* (n > 10 cells). (I) Time lapse of Rlc1-GFP (green) at 25°C in *cdc15^{19D}* cells. Separation of the SPB, marked by Sid4-mRFP (purple), was used as time reference. Arrowheads point to double ring structures. (J) Image of a double cytokinetic ring structure in meGFP-*cdc15^{16D}*. Error bars represent standard deviation. Bars, 5 µm.

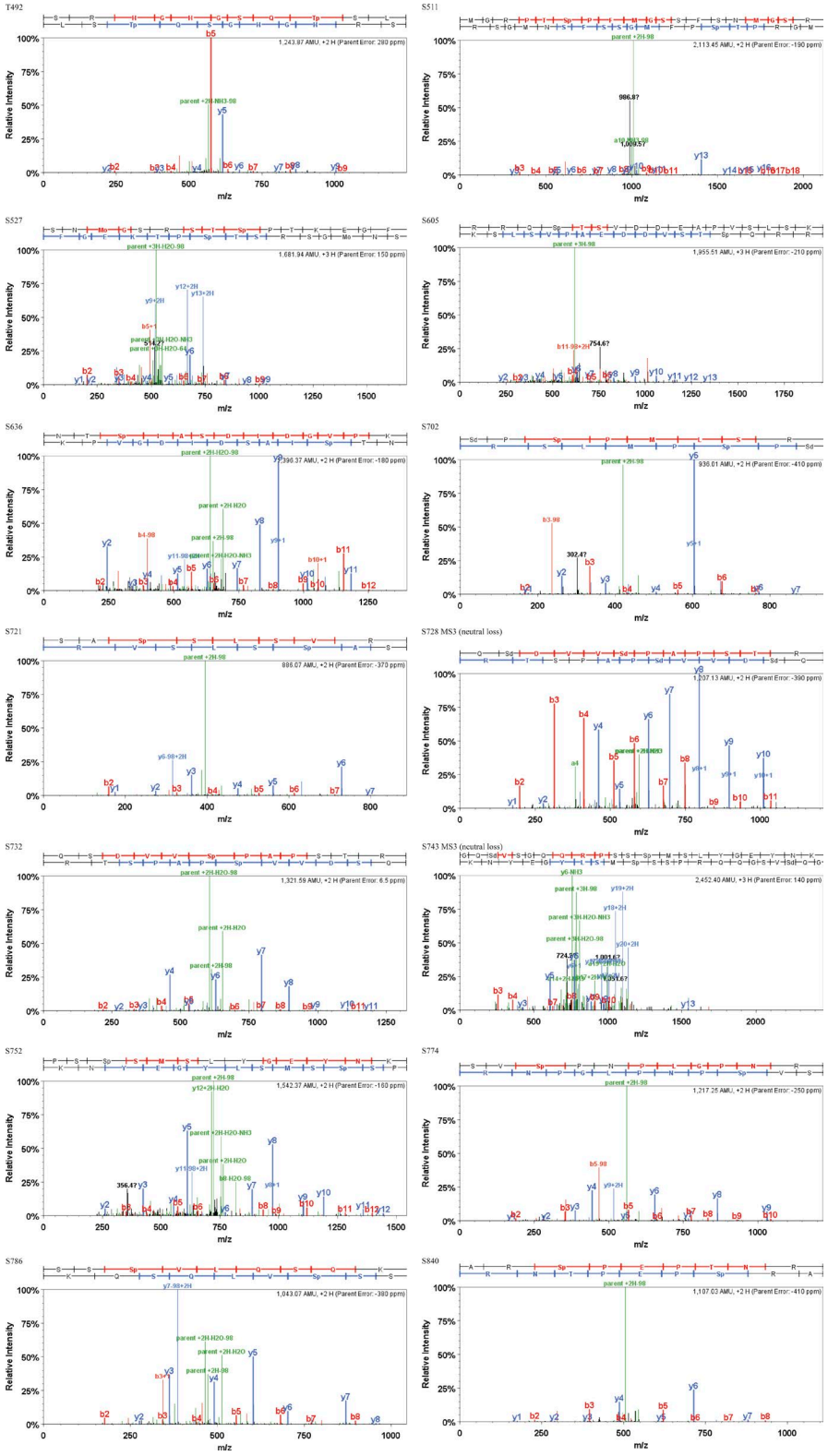

Figure S4. **Mass spectra of a representative phosphopeptide from each of the identified Pom1 phosphorylation sites on Cdc15.** These mass spectra were extracted from Scaffold PTM with matched b and y ions highlighted in red and blue, respectively. Ions resulting from neutral loss are highlighted in green. For most of the phosphorylation sites, both tandem mass spectometry (MS/MS; MS2) and MS/MS/MS (MS3; i.e., further MS/MS fragmentation of the ion that results from the neutral loss of phosphate of the parent ion during MS2 scan) spectra were acquired. In these cases, only MS2 spectra are shown here. For S728 and S743, the evidence of phosphorylation is only from MS3, probably because of the strong neutral loss of phosphate during MS2, resulting in a poor MS2 fragmentation. Mo, methionine with oxidation; Sd, serine with loss of water; Sp/Tp, phosphorylated serine/threonine.

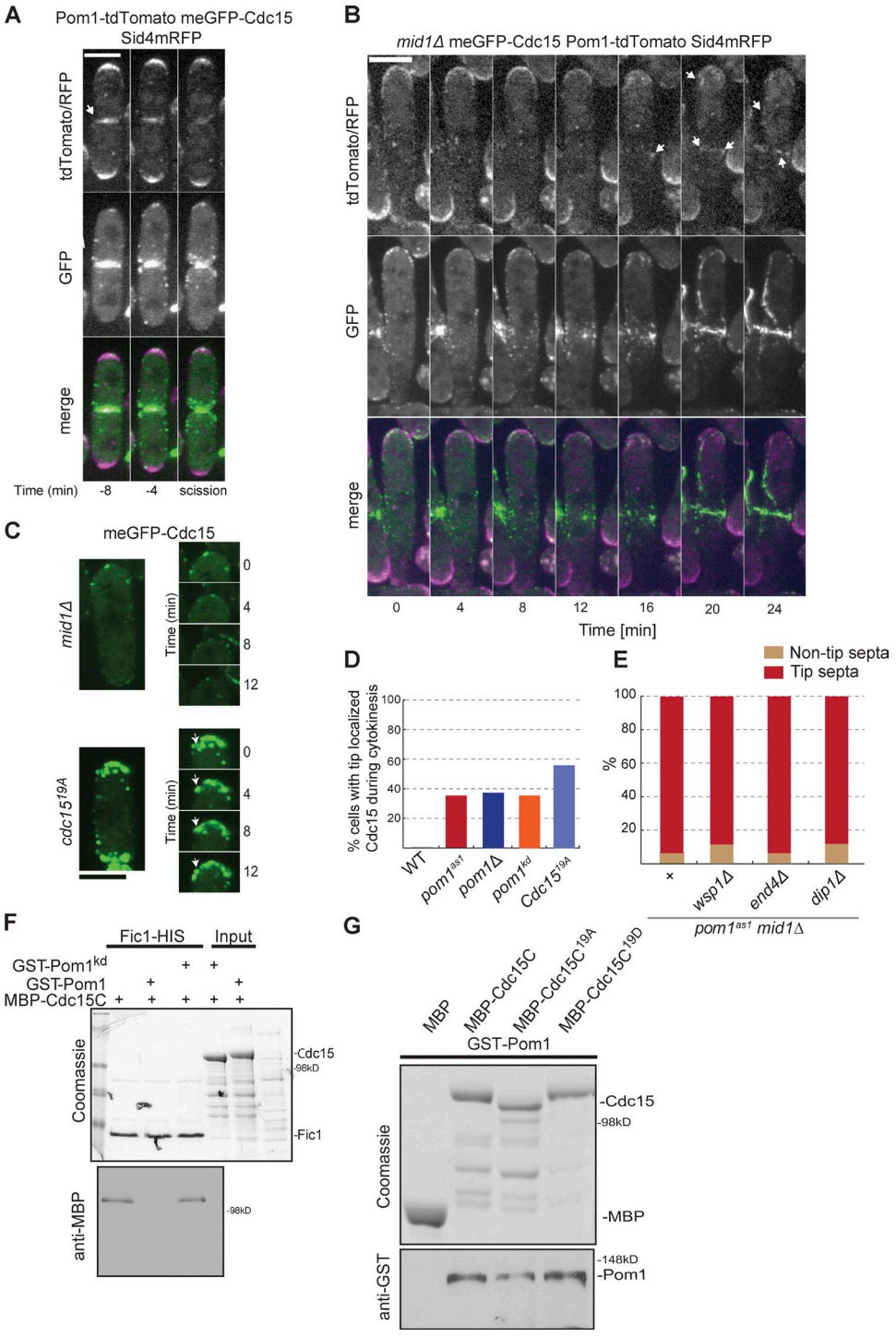

Figure S5. **Pom1 promotes Cdc15 dynamics in vivo and inhibits Cdc15 binding with Fic1 and Pxl1 in vitro.** (A) Localization of Pom1-tdTomato (purple) and meGFP-Cdc15 (green) at the septum. The SPB marker Sid4-mRFP (purple) was used as time reference. The arrow indicates presence of Pom1 in the septum. (B) meGFP-Cdc15 (green) and Pom1-tdTomato (purple) in *mid1Δ* cells assembling a cytokinetic ring at midcell. The SPB marker Sid4-mRFP was used as reference. Arrows point to Pom1 localization at the contractile ring, both at the medial division site and along strands forming from the cell pole. (C) meGFP-Cdc15 in *cdc15*^{19A} and *mid1Δ* cells. Arrows indicate stable GFP dots at the cell tips. Time is depicted on the vertical scale bar. (D) Quantification of the percentage of cells in cytokinesis (as defined by the presence of a Cdc15 ring) also displaying mEGFP-Cdc15 signal at cell tips ($n > 50$). (E) Actin patch mutants do not restore tip occlusion in *mid1Δ pom1*^{as1} cells. Cells of indicated genotypes were treated with 1 μM 3MB-PP1 at 25°C for 2 h, stained with calcofluor, and tip septa among septated cells quantified ($n > 300$). (F) Pom1 phosphorylation inhibits Cdc15-Fic1 interaction. Recombinant Fic1-His was immobilized on beads and incubated with recombinant MBP or MBP-Cdc15C, prephosphorylated or not by recombinant purified GST-Pom1 or GST-Pom1^{kd}. Beads were washed and bound proteins were run on SDS-PAGE and detected by Coomassie staining and Western blotting using anti-MBP antibodies. One fifth of each MBP protein input is shown as a control. (G) Constitutively hyperphosphorylated Cdc15 is still able to bind Pom1. In vitro binding assays between Pom1 and Cdc15 using recombinant MBP, MBP-Cdc15C, MBP-Cdc15^{19A}, and MBP-Cdc15^{19D}, incubated with recombinant GST and GST-Pom1. Amylose beads were washed and bound proteins were run on SDS-PAGE and detected by Coomassie staining (top) and anti-GST antibodies (bottom). Bars, 5 μm.

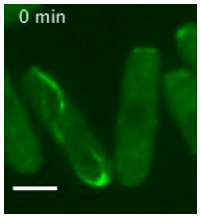

Video 1. **Actomyosin ring formation in *mid1Δ*.** Time lapse of meGFP-Cdc15 (green) in *mid1Δ* cells with images taken every 2 min for 80 min. The video is run at 3.6 frames per second. Note the sliding of the actomyosin ring in two cells with the Cdc15-marked ring assembling at the cell tips before sliding toward the cell middle. Bar, 5 µm.

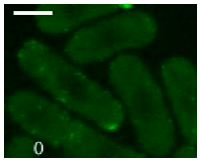

Video 2. **Actomyosin ring formation in *pom1^{as1} mid1Δ*.** Time lapse of meGFP-Cdc15 (green) in *pom1^{as1} mid1Δ* cells treated with 3MB-PP1 for 60 min before imaging. Images were taken every 4 min for 188 min and the movie is run at 3.6 frames per second. Note the inability of the actomyosin ring to slide toward the cell middle, with Cdc15 remaining attached to the cell poles. Note also the remarkable ability of the two strands of the ring originating from each cell pole to precisely meet. Bar, 5 µm.

Table S1. **List of strains used in this study**

Number	Genotype	Source
YSM1180	h- ade6-M210 leu1-32 ura4-D18	Lab Stock
YSM1182	h+ ade6-M216 leu1-32 ura4-D18	Lab Stock
YSM2627	h+ mid1::ura4+ ade6-M210 leu1-32	This study
YSM563	h+ pom1-as1 (T778G) ade6-M216 leu1-32 ura4-D18	Lab Stock
YSM2628	pom1-as1-tomato:: NatMXR mid1-366* ade6-M210 leu1-32 ura4-D18	This study
AR140	h- mEGFP-cdc15:: KanMX leu1-32 ura4-D18	Arasada and Pollard., 2011
MBY2331	h- cdc15-GFP::KanMX ade6-M210 leu1-32 ura4-D18	Huang et al., 2007
KG10025	h- cdc15-V5:: KanMX ade6-M210 leu1-32 ura4-D18	Roberts-Galbraith et al., 2010
YSM2629	ura4-294::nmt82-myo52N-RFP-nup146-ura4+ pom1-as1-tomato::NatMXR	This study
YSM2630	h+ pom1::KanMX; ura4-294::8nmt82-myo52N-GFP-nup146-ura4+ leu1-32 ura4-294	This study
YSM2631	h- ura4-294::nmt82-myo52N-RFP-nup146-ura4+ leu1-32 ura4-294	This study
YSM2632	h- pom1-as1-tomato::NatMX mid1::ura4+ ade6-M210 leu1-32	This study
YSM2633	h+ pom1-as1-tomato::NatMX mid1::ura4+ ade6-M210 leu1-32	This study
YSM2634	pom1-as1(T778G) mid1::ura4+ cdc15-GFP::KanMX ade6-M210 leu1-32	This study
YSM2635	cdc15-V5:: KanMX pom1-as1-tomato:: NatMX mid1:: ura4+ ade6-M210 leu1-32	This study
YSM2636	pom1-as1-tomato:: NatMX mid1:: ura4+ mEGFP-Cdc15:: KanMX ade6-M210 leu1-32	This study
YSM2637	pom1-as1-tomato:: NatMX cdc15 (SP11A)- V5:: KanMX mid1::ura4+ ade6-M210 leu1-32	This study
YSM2638	pom1-as1-tomato:: NatMX cdc15 (SP11D)- V5:: KanMX mid1::ura4+ ade6-M210 leu1-32	This study
YSM2639	h- pom1-as1-tomato:: NatMX cdc15 (RXXS13A)- V5:: KanMX mid1::ura4+ ade6-M210 leu1-32	This study
YSM2640	pom1-as1-tomato:: NatMX cdc15 (RXXS13D)- V5:: KanMX mid1::ura4+ ade6-M210 leu1-32	This study
YSM2641	cdc15 (RXXS13A)- V5:: KanMX mid1:: ura4+ ade6-M210 leu1-32	This study
YSM2642	cdc15-GFP-KanMX ura4-294::nmt82-myo52N-GFP-nup146-ura4+ leu1-32	This study
YSM2643	pom1::KanMX cdc15-GFP-KanMX; ura4-294::nmt82-myo52N-GFP-nup146-ura4+ leu1-32	This study
YSM2644	pom1::KanMX cdc15(RXXS13D)-V5-KanMX ura4-294::nmt82-myo52N-GFP-nup146-ura4+ leu1-32	This study
YSM2645	mEGFP-cdc15-KanMX pom1::KanMX; ura4-294::nmt82-myo52N-RFP-nup146-ura4+ leu1-32	This study
YSM2646	h+ mEGFP-Cdc15::KanMX sid4mRFP:: ura4+ ade6-M21X leu1-32	This study
YSM2647	mEGFP-Cdc15::KanMX sid4mRFP:: ura4+ pom1::ura4+ ade6M21X leu1-32	This study
YSM2648	mEGFP-Cdc15::KanMX sid4mRFP:: ura4+ mid1::ura4+ ade6M21X leu1-32	This study
YSM2649	mEGFP-Cdc15::KanMX sid4mRFP:: ura4+ mid1::ura4+ ade6M21X leu1-33	This study
YSM2650	pom1-as1-tomato::NatMX mEGFP-Cdc15::KanMX sid4-mRFP::ura4+ ade6-M210 leu1-32	This study
YSM2651	h+ Rlc1-GFP::KanMX sid4-mRFP::ura4+ ade6-M210 leu1-32	This study
YSM2652	Rlc1-GFP::KanMX sid4-mRFP::ura4+ pom1::ura4+ ade6? leu1-32	This study
YSM2653	h- pom1-as1-tomato:: NatMX Rlc1-GFP::KanMX sid4-mRFP::ura4+ ade6-M216 leu1-32	This study
YSM2654	cdc15-V5:: KanMX pom1as1-Tomato:: NatMX ade6-M210 leu1-32 ura4-D18	This study
YSM2655	h+ Cdc15-V5:: KanMX pom1:: ura4+ ade6-M210 leu1-32	This study
YSM2656	cdc15 (SP11A)- V5:: KanMX mid1:: ura4+ ade6-M210 leu1-32	This study
YSM2657	pom1-as1-tomato:: NatMX sid4-mRFP::ura4+ mEGFP-Cdc15:: KanMX mid1::ura4+ ade6-M216 leu1-32	This study
YSM2658	mid1::ura4+ KanMX:: mEGFP-Cdc15-19A ade6-M216 leu1-32	This study
YSM2659	h- pom1-as1-tomato:: NatMX Rlc1-GFP::KanMX cdc15 (RXXS13D)- V5:: KanMX sid4mRFP:: ura4+ leu1-32	This study
YSM2660	pom1-as1-tomato:: NatMX Rlc1-GFP::KanMX cdc15 (RXXS13D)- V5:: KanMX sid4mRFP:: ura4+ mid1:: ura4+ leu1-32	This study
YSM2661	pom1-as1-tomato:: NatMX Rlc1-GFP::KanMX cdc15 (19D)- V5:: KanMX sid4mRFP:: ura4+ mid1:: ura4+ leu1-32	This study
YSM2662	h- cdc15-19A ade6-M216 leu1-32	This study
YSM2663	h- cdc15-19D ade6-M216 leu1-32	This study
YSM2664	h- cdc15-19A-V5:: KanMX ade6-M216 leu1-32	This study
YSM2665	h- cdc15-19D-V5:: KanMX ade6-M216 leu1-32	This study
YSM2666	cdc15-19A-V5:: KanMX mid1::ura4+ ade6-M216 leu1-32	This study
YSM2667	cdc15-19D-V5:: KanMX mid1::ura4+ ade6-M216 leu1-32	This study
YSM2668	h- KanMX:: mEGFP-Cdc15-19A ade6-M216 leu1-32 ura4-D18	This study
YSM2669	h- KanMX:: mEGFP-Cdc15-19D ade6-M216 leu1-32 ura4-D18	This study
YSM2670	cdc15-19D-V5::KanMX Rlc1-GFP:: KanMX sid4mRFP::ura4+ ade6-M216 leu1-32	This study
YSM2671	h+ pom1-tomato:: NatMX mEGFP-Cdc15::KanMX sid4mRFP:: ura4+ ade6-M216 leu1-32	This study
YSM2672	mid1::ura4+ pom1-tomato:: NatMX mEGFPCdc15::KanMX sid4mRFP:: ura4+ ade6-M216 leu1-32	This study
YSM2673	cdc25-22 pom1-as1 (T778G) sid4-mRFP::ura4+ mEGFP-Cdc15:: KanMX ade6-M216 leu1-32	This study
YSM2674	pom1-as1 pxl1:: ura4+ mid1:: KanMX ade6-M210 leu1-32	This study
YSM2675	pom1-as1-tomato:: NatMX mid1:: KanMX fic1:: ura4+ leu1-32	This study
YSM2676	pom1-as1-tomato::NatMX mid1::ura4+ dip1::NatMX	This study
YSM2677	pom1-as1-tomato::NatMX mid1::ura4+ end4::ura4+ ade6-M216 leu1-32	This study
YSM2678	pom1-as1-tomato::NatMX mid1::ura4+ wsp1Δ::kanMX6 ade6-M216 leu1-32	This study
YSM2679	cdc15 (RXXS13A)- V5:: KanMX mid1:: ura4+ pxl1Δ::ura4+	This study

Table S1. **List of strains used in this study** *(Continued)*

Number	Genotype	Source
YSM2680	cdc15-19A-V5:: KanMX pxl1Δ::ura4+ ade6-M21X leu1-32	This study
YSM2681	cdc15 (RXXS13A)- V5:: KanMX mid1:: ura4+ fic1:: ura4+ leu1-32	This study
YSM2682	cdc15-19A- V5:: KanMX mid1:: ura4+ fic1:: ura4+ leu1-32	This study
YSM2683	h+ fic1-GFP::KanMX sid4-mRFP:.Ura4+ ade6-M216 leu1-32	This study
YSM2684	h- fic1-GFP::KanMX sid4-mRFP:.Ura4+ pom1-as1-tomato leu1-32	This study
YSM2685	fic1-GFP::KanMX sid4-mRFP:.Ura4+ cdc15-19A-V5:: KanMX ade6-M210 leu1-32	This study
YSM2686	fic1-GFP::KanMX sid4-mRFP:.Ura4+ cdc15-19D-V5:: KanMX ade6-M210 leu1-32	This study
YSM2687	cdc25-22 fic1-GFP::KanMX sid4-mRFP:.ura4+ pom1-as1-Tomato:: NatMX leu1-32	This study
YSM2688	pxl1-5Gly(linker)-GFP:: ura4+ cdc15-19D-V5::KanMX ade6-M216 leu1-32	This study
YSM2689	fic1::ura4+ mEGFP-Cdc15::KanMX sid4mRFP:: ura4+ ade6-M216 leu1-32	This study
YSM2690	pxl1Δ::ura4+ sid4-mRFP::ura4+ meGFP-cdc15:: KanMX ade6-M216 leu1-32	This study
YSM2691	h- cps1-191 ura4-D18	Le Goff et al., 1999
YSM2692	pom1-as1-tomato:: NatMX mid1:: KanMX cps1-191 ade6-M216 leu1-32 ura4-D18	This study
YSM2693	cdc15-19A-V5:: KanMX pom1-as1-tomato:: NatMX mid1::ura4+ ade6-M216 leu1-32	This study
YSM2694	cdc15-19D-V5:: KanMX pom1-as1-tomato:: NatMX mid1::ura4+ ade6-M216 leu1-32	This study
YSM2695	mEGFP-Cdc15-19A:: KanMX Sid4mRFP:: ura4+ ade6-M216 leu1-32	This study
YSM2696	pom1-2:: KanMX mEGFP-cdc15 sid4-mRFP:: ura4+	This study
YSM2697	rlc1-GFP::KanMX sid4-mRFP::Ura4+ pom1-2-GFP::KanMX ade6-M216 leu1-32	This study
YSM2698	clp1::ura4+ pom1-as1-tomato::NatMX mid1::ura4+ ade6-M21X leu1-32	This study
YSM2736	h- KanMX:: mEGFP-Cdc15-16D ade6-M216 leu1-32 ura4-D18	This study
YSM2737	h- cdc15-16D-V5:: KanMX ade6-M216 leu1-32	This study
YSM2738	cdc15-16D-V5:: KanMX pom1-as1-tomato:: NatMX mid1::ura4+ ade6-M216 leu1-32	This study
YSM2739	pxl1-5Gly(linker)-GFP:: ura4+ cdc15-16D-V5::KanMX ade6-M216 leu1-32	This study

References

Arasada, R., and T.D. Pollard. 2014. Contractile ring stability in *S. pombe* depends on F-BAR protein Cdc15p and Bgs1p transport from the Golgi complex. *Cell Reports.* 8:1533–1544. http://dx.doi.org/10.1016/j.celrep.2014.07.048

Huang, Y., T.G. Chew, W. Ge, and M.K. Balasubramanian. 2007. Polarity determinants Tea1p, Tea4p, and Pom1p inhibit division-septum assembly at cell ends in fission yeast. *Dev. Cell.* 12:987–996. http://dx.doi.org/10.1016/j.devcel.2007.03.015

Le Goff, X., A. Woollard, and V. Simanis. 1999. Analysis of the cps1 gene provides evidence for a septation checkpoint in Schizosaccharomyces pombe. *Mol. Gen. Genet.* 262:163–172. http://dx.doi.org/10.007/s004380051071105035 48

Roberts-Galbraith, R.H., and K.L. Gould. 2010. Setting the F-BAR: Functions and regulation of the F-BAR protein family. *Cell Cycle.* 9:4091–4097. http://dx.doi.org/10.4161/cc.9.20.13587